Diffusive Noise Controls Early Stages of Genetic Demixing

Rashmiranjan Bhutia, Stephy Jose, Prasad Perlekar, and Kabir Ramola
Tata Institute of Fundamental Research, Hyderabad, 500046, India

(Received 5 June 2025; accepted 28 July 2026; published 26 August 2026)

Theoretical descriptions of the stepping-stone model, a cornerstone of spatial population genetics, have long overlooked diffusive noise arising from migration dynamics. We derive a fluctuating hydrodynamic description of this model from microscopic rules, which we then use to demonstrate that diffusive noise significantly alters early-time genetic demixing, which we characterize through heterozygosity, a key measure of diversity. Combining macroscopic fluctuation theory and microscopic simulations, we demonstrate that the scaling of allele-number fluctuations in a spatial domain displays an early-time behavior dominated by diffusive noise. Our results underscore the need for additional terms in existing continuum theories and highlight the necessity of including diffusive noise in models of spatially structured populations.

DOI: 10.1103/xmbp-d85n

Understanding how genetic diversity is generated and maintained in spatially structured populations is a fundamental problem in evolutionary biology [1–6]. Spatial population genetics, epitomized by the stepping-stone model [7,8], provides a framework to study allele dynamics across discrete demes connected by migration and has been successful in quantitatively capturing fixation times and genetic drift in spatially evolving populations [8,9]. Despite its utility, classical theories [1,7] and modern continuum approaches [8,10,11] have emphasized drift, selection, and local demographic noise, while largely overlooking stochastic fluctuations arising from migration (diffusive noise). This omission matters because migration rates can exceed birth-death rates in natural populations [12–15], making diffusive noise potentially dominant. Coarse-grained hydrodynamic descriptions, such as the stochastic Fisher-Kolmogorov-Petrovsky-Piscounov (sFKPP) equation [8,10,11,16], are often used to interpret the stepping-stone model, but are commonly obtained phenomenologically or by coarse graining. Recent derivations of fluctuating hydrodynamics for related systems likewise omitted diffusive noise [5,8,17,18], implicitly assuming reaction-driven fluctuations dominate. More broadly, diffusive noise is known to strongly modify dynamics and phase behavior in other microscopic systems [19–23].

In this Letter, we address this gap by deriving a fluctuating hydrodynamic equation that incorporates both diffusive and reaction (demographic) noise. Our approach builds upon recent advancements in fluctuating hydrodynamics [20,24–26], which have successfully modeled microscopic fluctuations in systems with both diffusive and reactive dynamics. While reaction-diffusion descriptions with both conservative diffusive noise and nonconservative demographic noise have been studied [27–32], they are typically phenomenological and assume conservative noise with linear density dependence. In contrast, our formulation derives the noise directly from the microscopic stepping-stone dynamics with fixed local population size, leading to a nonlinear multiplicative noise structure that follows from binary-allele competition together with local particle conservation. We illustrate the significant effects of this diffusive noise by computing the heterozygosity as well as density fluctuations, and show how this is a much more accurate framework for understanding microscopic simulations as well as experiments. Crucially, we show that the early-time behavior of genetic demixing, quantified by heterozygosity at the origin, is well described by a modified hydrodynamic equation and not by the ubiquitously used sFKPP framework [8,11,33].

Stepping-stone model—We consider a one-dimensional stepping-stone model (see Fig. 1) consisting of a periodic lattice of length $l = La$, with lattice sites indexed by $i = -L/2+1, \ldots, -1, 0, 1, \ldots, L/2$ and separated by a distance a. Each site represents a deme that contains a fixed number N of individuals belonging to two allelic types, denoted A and B. The system evolves through local reproduction and short-range migration processes, which are modeled using discrete-time update rules.

At each time step, the following processes can occur. The first is reproduction, in which two individuals are randomly selected within a deme, and one of them reproduces while the other is removed, maintaining the population size N at each site fixed. Reproduction is modeled by the following reactions [34]:

$$A + B \xrightarrow{K_1} A + A, \qquad A + B \xrightarrow{K_2} B + B, \tag{1}$$

where K_1 and K_2 are the rates of reproduction of alleles A and B, respectively.

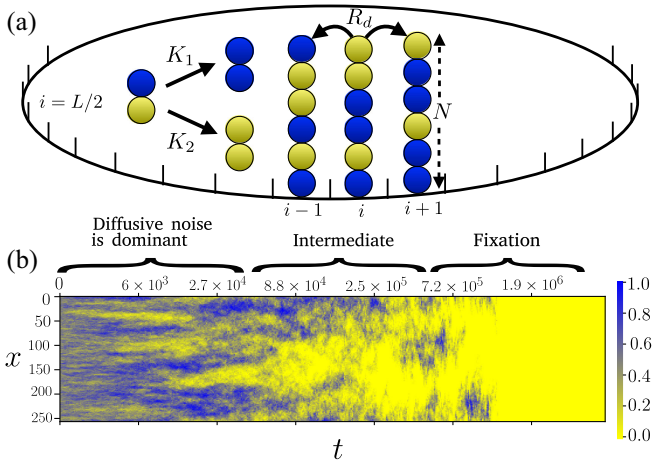

FIG. 1. (a) Schematic of the one-dimensional stepping-stone model. Lattice sites indexed by i represent islands (demes), each with N individuals of two types: A (blue) and B (yellow). (b) Time evolution of the frequency $f_i = n_i^A/N$ shows three regimes: an early well-mixed phase where diffusion and diffusive noise dominate observables; an intermediate, reaction-driven genetic demixing phase where distinct allele domains form and diffusive noise affects domain boundaries; and a late fixation phase, when domains reach system size and a single allele occupies the entire system.

The second process is migration, in which, with rate R_d, an individual at site i is exchanged with an individual from a neighboring site $i+1$. This model includes stochastic effects due to genetic drift, leading to fixation dynamics and spatial heterogeneity in allele frequencies. The key observable of interest is the fraction $f_i(\tau_j)$ of allele A at site i at time step τ_j, which evolves under the combined influence of reactions and diffusion. This is defined as $f_i(\tau_j) = n_i^A/N$, where n_i^A is the number of A alleles. The fraction of allele B is then simply given by $1 - f_i(\tau_j)$, since the total number of individuals per site is conserved. We assume a fixed number of individuals per deme, as in classical spatial population genetics models [7], which can represent a constant local carrying capacity set by resources or competition. Our simulations employ the same microscopic rules, whose details as well as additional explanations related to the figures in the main text are provided in Supplemental Material [35].

Derivation of fluctuating hydrodynamics—To derive the fluctuating hydrodynamics of the stepping-stone model, we start from the discrete description and extend it to a continuum framework [38–40]. The change in allele frequency at site i during a microscopic time step $d\tau$ is captured by the quantity $J_i(\tau_j) = f_i(\tau_{j+1}) - f_i(\tau_j)$, which we refer to as the "microscopic current." The probability of observing a specific trajectory of frequencies $\{f_i(\tau_j)\}$ can be expressed in terms of these currents as

$$P(\{f\}) = \left\langle \prod_{i,j} \delta(f_i(\tau_{j+1}) - f_i(\tau_j) - J_i(\tau_j)) \right\rangle_{\{J\}}, \quad (2)$$

where the delta functions enforce the dynamical rules, and the average is taken over all possible realizations (or histories) of $\{J\}$. Next, using the integral representation of the delta function, $\delta(a-b) = \int_{-i\infty}^{i\infty} [(d\hat{f})/(2\pi i)]\, e^{-\hat{f}(a-b)}$, the probability of observing a trajectory is rewritten as a path integral over auxiliary fields $\hat{f}_i(\tau_j)$ as

$$P(\{f\}) = \int \mathcal{D}\hat{f} e^{-S}. \quad (3)$$

Here, $\mathcal{D}\hat{f} = \prod_{i=-L/2+1}^{L/2} \prod_{j=1}^{M} d\hat{f}_i(\tau_j)$ denotes the path integral measure over the auxiliary fields at each site i and time step τ_j and the action S is given by

$$S = \sum_{i,j} \left[\hat{f}_i(\tau_j)(f_i(\tau_{j+1}) - f_i(\tau_j)) \right] \underbrace{- \ln \left[\prod_j \langle e^{\sum_i \hat{f}_i(\tau_j) J_i(\tau_j)} \rangle \right]}_{(T_d + T_r)}. \quad (4)$$

Equation (4) holds for any process governed by a microscopic stochastic rule, whereas the specific form of the second term depends on the underlying process. This path-integral approach provides a systematic framework to derive the continuum limit. Given that the probability of each event is known, the calculation of the average in Eq. (4) becomes straightforward. The second term of the above action has been divided into contributions from two sources, T_d and T_r, which can be derived from the microscopic rules of the stepping-stone model (see Ref. [35] for a detailed derivation). The diffusive part T_d, which arises from particle exchanges between neighboring sites i and $i+1$, is given as

$$T_d = R_d d\tau \sum_{i,j} \left\{ f_i(\tau_j)[1 - f_{i+1}(\tau_j)] \left(e^{\frac{\hat{f}_{i+1}(\tau_j) - \hat{f}_i(\tau_j)}{N}} - 1 \right) + f_{i+1}(\tau_j)[1 - f_i(\tau_j)] \left(e^{\frac{\hat{f}_i(\tau_j) - \hat{f}_{i+1}(\tau_j)}{N}} - 1 \right) \right\}. \quad (5)$$

A similar expression for T_d has been reported for the weakly asymmetric simple exclusion process [41,42] as well as for other related models [23,26]. The reaction term T_r, which captures birth-death processes within a deme, is given as

$$T_r = d\tau \sum_{i,j} \Big\{ K_1 f_i(\tau_j)[1 - f_i(\tau_j)] \Big(e^{\frac{\hat{f}_i(\tau_j)}{N}} - 1 \Big) + K_2 f_i(\tau_j)[1 - f_i(\tau_j)] \Big(e^{-\frac{\hat{f}_i(\tau_j)}{N}} - 1 \Big) \Big\}. \quad (6)$$

We next use this form of the action to derive the continuum fluctuating hydrodynamic equation for the stepping-stone model. To do so, we perform a coarse-graining procedure [38]. The spatial and temporal coordinates are scaled as $x = ia$ and $t = jd\tau$, with $a, d\tau \to 0$. To ensure hydrodynamic scaling, the exchange rate R_d is rescaled as $R_d \to \tilde{R}_d/a^2$, ensuring that diffusive noise and reaction noise contribute equally in the hydrodynamic limit. Since the migration rate scales as $R_d \propto a^{-2}$, migration occurs on timescales much shorter than those associated with the evolution of the coarse-grained density field. Rapid migration therefore induces local equilibration across neighboring sites within a mesoscopic region before significant reactions occur. In this limit, the local distribution approaches a factorized product measure across sites, with each deme characterized by a binomial distribution conditioned on the local allele frequency, $P_{\mathrm{eq}}[n_i^A | f_i(t)] = \mathrm{Binomial}[n_i^A; N, f_i(t)]$. Furthermore, since each deme contains N individuals, the variables $f_i = n_i^A/N$ are themselves locally averaged quantities. Consequently, connected nearest-neighbor correlations are suppressed in the large-N limit, $\langle f_i f_{i+1} \rangle = \langle f_i \rangle \langle f_{i+1} \rangle + \mathcal{O}(1/N)$, which yields the asymptotic factorization $[\langle f_i(\tau_j)(1 - f_{i+1}(\tau_j))] \rangle \simeq f_i(\tau_j)[1 - f_{i+1}(\tau_j)]$ up to subleading corrections from short-range correlations and spatial gradients [23,26,38,43–46]. We next expand the discrete fields $f_{i\pm1}(\tau_j)$ and $\hat{f}_{i\pm1}(\tau_j)$ in Taylor series: $f(x \pm a, t) \approx f(x,t) \pm a\partial_x f + (a^2/2)\partial_x^2 f$, and $\hat{f}(x \pm a, t) \approx \hat{f}(x,t) \pm a\partial_x \hat{f} + (a^2/2)\partial_x^2 \hat{f}$, and substitute into the action S. Here, $f(x,t)$ is the continuous representation of the allele fraction. Retaining terms up to $\mathcal{O}(a^2, d\tau)$, we find that the action separates into contributions from diffusion and reactions as

$$S = \frac{1}{a} \int dx dt \Big[\hat{f}\partial_t f + D_d \partial_x f \partial_x \hat{f} - \frac{\sigma_s}{2} \hat{f} - \frac{\sigma_d}{2} (\partial_x \hat{f})^2 - \frac{\sigma_r}{2} \hat{f}^2 \Big], \quad (7)$$

where $D_d = \tilde{R}_d/N$ is the macroscopic diffusion constant, while $\sigma_d = 2D_d f(1-f)/N$, $\sigma_r = 2D_r f(1-f)/N$ and $\sigma_s = 2Sf(1-f)/N$ are noise amplitudes associated with diffusion, reaction, and selection (deterministic drift) respectively. In addition, $D_r = R_r/N$, $R_r = (K_1 + K_2)/2$, and $S = K_1 - K_2$ represent the genetic diffusion constant, neutral reaction rate, and selective advantage, respectively. Next, following standard techniques [38,47–49], we employ a Hubbard-Stratonovich transformation so that the quadratic terms in $\hat{f}$ are linearized by introducing Gaussian noise fields $\eta_d(x,t)$ (conservative) for the diffusive term $(\sigma_d/2)(\partial_x \hat{f})^2$ and $\eta_r(x,t)$ (nonconservative) for the reaction term $(\sigma_r/2)\hat{f}^2$. This yields the probability of observing a history of allele frequencies as

$$P(\{f\}) = \int \mathcal{D}\hat{f} D\eta_d D\eta_r e^{-S}, \quad (8)$$

where $\int \mathcal{D}\hat{f} D\eta_d D\eta_r$ denotes the path integral measure over the auxiliary fields $\hat{f}(x,t)$, and the noise fields $\eta_d(x,t)$ and $\eta_r(x,t)$, at each space-time point and

$$S = \frac{1}{a} \int dx dt [\hat{f}\partial_t f - \hat{f} D_d \partial_x^2 f - \hat{f}\partial_x(\sqrt{\sigma_d}\eta_d) - \hat{f}\frac{\sigma_s}{2} - \hat{f}\sqrt{\sigma_r}\eta_r + \frac{\eta_d^2}{2} + \frac{\eta_r^2}{2}]. \quad (9)$$

Performing an integral over $\hat{f}$, we obtain

$$P(\{f\}) \approx \int D\eta_d D\eta_r e^{-\frac{1}{2a}\int dx dt(\eta_d^2 + \eta_r^2)} \times \delta\Big(\partial_t f - D_d \partial_x^2 f - \frac{\sigma_s}{2} - \partial_x(\sqrt{\sigma_d a}\eta_d) - \sqrt{\sigma_r a}\eta_r \Big). \quad (10)$$

This leads to the stochastic partial differential equation,

$$\partial_t f = D_d \partial_x^2 f + \frac{S}{N} f(1-f) + \partial_x(\sqrt{\sigma_d a}\eta_d) + \sqrt{\sigma_r a}\eta_r, \quad (11)$$

where η_d and η_r are Gaussian white noises with mean zero and correlations given by

$$\langle \eta_\alpha(x_1,t_1)\eta_\beta(x_2,t_2) \rangle = \delta_{\alpha\beta}\delta(x_1 - x_2)\delta(t_1 - t_2), \quad (12)$$

where $\alpha, \beta \equiv d,\ r$ represent the diffusive and reaction noises respectively. Equation (11) is a central result of this Letter. We note that this equation without the presence of the third term is popularly known as the sFKPP equation [8,10,11,16], which is a common model to describe the invasion of advantageous organisms within an existing population. To highlight the effects of diffusive noise, we focus on the case where the selective advantage is zero, i.e., we set the second term in Eq. (11) to zero. This allows us to isolate and study the impact of stochastic effects due to migration and genetic drift in detail.

Effect on heterozygosity—To illustrate the consequences of the diffusive noise, we focus on the two-point correlation function $H(x_1, x_2, t) = \langle f(x_1,t)[1 - f(x_2,t)] + f(x_2,t)[1 - f(x_1,t)] \rangle$, commonly referred to as the average spatial heterozygosity in population genetics. This represents the

average probability that two individuals at positions x_1 and x_2 carry different alleles and is routinely used to quantify genetic diversity [7,8,33]. Starting from the fluctuating hydrodynamic equation for the frequency of the allele given in Eq. (11), we derive the equation for H. Following previous work [8], we apply Ito's Lemma, and expand H to second order in δf, using the stochastic increments $\delta f(x,t) = D_d \partial_x^2 f \delta t + dw(x,t)$, where dw encodes the noise correlations, and have

$$\langle dw(x,t)dw(x',t')\rangle = \left(\frac{2D_d a}{N}\partial_x \partial_{x'}[f(1-f)\delta(x-x')] + \frac{2D_r a}{N} f(1-f)\delta(x-x')\right) \times \delta(t-t'). \quad (13)$$

An analogous form of averaging arises in general Langevin processes describing systems with diffusive dynamics [50]. After averaging over the noise, the deterministic terms yield $D_d(\partial_{x_1}^2 + \partial_{x_2}^2)H$, while the noise contributions produce $-[(2D_r a)/N]H\delta(x_1 - x_2)$ and $+[(2D_d a)/N]\partial_{x_1}\partial_{x_2}[H\delta(x_1 - x_2)]$, respectively. The first term reflects reaction-driven diversity loss as seen in previous studies [4,8,33], while the second term represents a new contribution arising from diffusive noise. The resulting equation for the heterozygosity $H(x_1, x_2)$ becomes

$$\partial_t H = 2D_d \partial_x^2 H - \frac{2D_r a}{N} H\delta(x) + \frac{2D_d a}{N}\partial_x^2[H\delta(x)], \quad (14)$$

where $x = x_1 - x_2$. This generalizes previous equations that did not include diffusive noise [8]. Our modified equation introduces an additional term, the third term arising uniquely from diffusive noise, which modifies the spatial structure of heterozygosity. Specifically, it suppresses diversity at the origin while enhancing it at other spatial locations at short distances. This behavior is illustrated by the heterozygosity profiles shown in Fig. 2. We observe a clear discrepancy between Monte Carlo simulations and the theory without diffusive noise. However, when diffusive noise is correctly accounted for, the simulations match the theory perfectly. Previous theories without diffusive noise do not capture this, leading to discrepancies in spatial profiles when $R_r \ll R_d$. This analysis shows that early genetic demixing is accurately described by a hydrodynamic equation with diffusive noise rather than the sFKPP equation. However, the long-time behavior remains the same regardless of the presence of diffusive noise (see Supplemental Material for details [35]).

Number fluctuations in a finite domain—To further demonstrate the importance of diffusive noise, we next focus on an additional quantity, namely the fluctuations in the number of alleles across a spatial domain. The total flux of particles Q_T across the origin up to a time T has become

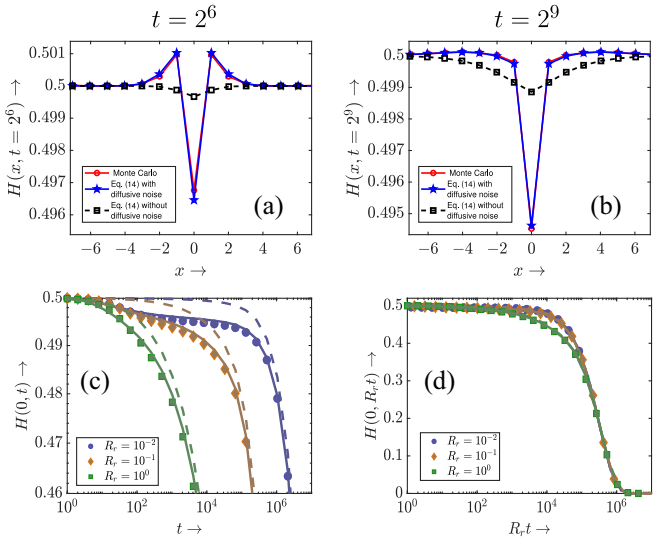

FIG. 2. Effect of diffusive noise on spatial heterozygosity $H(x,t)$. (a),(b) $H(x,t)$ at different times. Red circles are Monte Carlo data for the stepping-stone model; stars are solutions of Eq. (14) with diffusive noise; squares are solutions without it. (c) Time evolution of $H(0,t)$ for various reaction rates. Points are Monte Carlo results; solid and dashed lines are solutions of Eq. (14) with and without diffusive noise, respectively. (d) shows the long-time decay of heterozygosity for different reaction rates, with time rescaled by the reaction rate. All curves have the same large-time asymptotic behavior [35].

a standard observable in diffusive systems, both in and out of equilibrium, over the past few decades [22,24,51–57]. It is most commonly used as a test of large deviations using macroscopic fluctuation theory (MFT) [49,51,58–62]. In the following, we use this quantity to determine the relative contribution of diffusive noise in the stepping-stone model. We define the net change in allele concentration A up to time T in half the spatial domain (which includes contributions from both flux and reactions),

$$Q_T = \frac{1}{a}\int_0^{l/2}[f(x,T) - f(x,0)]dx. \quad (15)$$

The variance of Q_T, denoted $\langle Q_T^2\rangle_c$, provides insight into the fluctuations in allele transport within the system. Remarkably, we note that $\langle Q_T^2\rangle_c$ can be related to the heterozygosity H for uniform initial conditions. Assuming an initial frequency f_0 (see Supplemental Material [35]),

$$\langle Q_T^2\rangle_c = \iint_{\Omega\times\Omega}\left[f_0(1-f_0) - \frac{1}{2}H(x,y,T)\right]dxdy. \quad (16)$$

To compute this variance theoretically, we employ the MFT framework, which facilitates the analysis of fluctuations in systems governed by hydrodynamic equations [58]. Within the MFT framework, the probability of observing a specific trajectory of the system is characterized by an

action functional $\mathcal{S}$. This action $\mathcal{S}$ is the same as Eq. (9) but now biased by an extra term λq_T, i.e., $\mathcal{S} = S - \lambda q_T$. The moment generating function for Q_T, $\langle e^{\lambda Q_T}\rangle$, can be expressed as a path integral,

$$\langle e^{\lambda Q_T}\rangle = \int \mathcal{D}f\mathcal{D}\hat{f} e^{-L\mathcal{S}}, \tag{17}$$

where $\hat{f}$ is the conjugate field, and $q_T = \int_0^{1/2} [f(x',T) - f(x',0)]dx'$. To evaluate this path integral, we apply a saddle-point approximation [51]. The saddle-point approximation is valid because of the large prefactor L in front of the action, and becomes exact in the $L \to \infty$ limit. This leads to a set of coupled Euler-Lagrange equations for the fields $f(x,t)$ and $\hat{f}(x,t)$,

$$\begin{aligned}\partial_t f &= D_d\partial_x^2 f - \partial_x\left(\sigma_d(f)\partial_x\hat{f}\right) + \sigma_r(f)\hat{f},\\ \partial_t\hat{f} &= -D_d\partial_x^2\hat{f} - \frac{\sigma_d'(f)}{2}(\partial_x\hat{f})^2 - \frac{\sigma_r'(f)}{2}\hat{f}^2.\end{aligned} \tag{18}$$

Here, the primes denote derivatives with respect to f.

Next, we apply a standard perturbative expansion to compute the allele number fluctuations [22,51]. We expand both fields in powers of the perturbation parameter λ, which quantifies deviations from the typical trajectory,

$$f = f_0 + \lambda f_1 + \lambda^2 f_2 + \cdots, \qquad \hat{f} = \lambda\hat{f}_1 + \lambda^2\hat{f}_2 + \cdots. \tag{19}$$

At linear order in λ, the Euler-Lagrange equations become

$$\begin{aligned}\partial_t f_1 &= D_d\partial_x^2 f_1 - \partial_x\left(\sigma_d(f_0)\partial_x\hat{f}_1\right) + \sigma_r(f_0)\hat{f}_1,\\ \partial_t\hat{f}_1 &= -D_d\partial_x^2\hat{f}_1.\end{aligned} \tag{20}$$

The boundary conditions are $f_1(x,0) = 0$ (quenched initial state) and $\hat{f}_1(x,T) = \theta(x)$ [22,24,62], where $\theta(x) = 1$ for $x \in [0,1/2]$. The homogeneous solution for $\hat{f}_1$, backward in time ($\tau = T - t$), can be easily found in Fourier space to be

$$\hat{f}_1(k,\tau) = \frac{i(1-e^{ik\pi})}{2k\pi} e^{-D_d(2\pi k)^2\tau}. \tag{21}$$

At leading order (λ^2), the variance $\langle Q_T^2\rangle_c$ becomes

$$\langle Q_T^2\rangle_c = \sum_{k=-\infty}^{\infty}\int_0^T dt\left[\sigma_d k^2|\hat{f}_1(k,t)|^2 + \sigma_r|\hat{f}_1(k,t)|^2\right], \tag{22}$$

where $\hat{f}_1(k,t)$ given in Eq. (21) solves the linearized MFT equations in Eq. (20). The predictions from the above expression are compared with the results from direct numerical simulations of the stepping-stone model in Fig. 3, showing perfect agreement. As shown in the inset of Fig. 3, the above results are in excellent agreement with $\langle Q_T^2\rangle_c$ computed directly from the heterozygosity through Eq. (16). Thus the impact of diffusive noise on heterozygosity is easily detectable and accurately predicted by continuum theory.

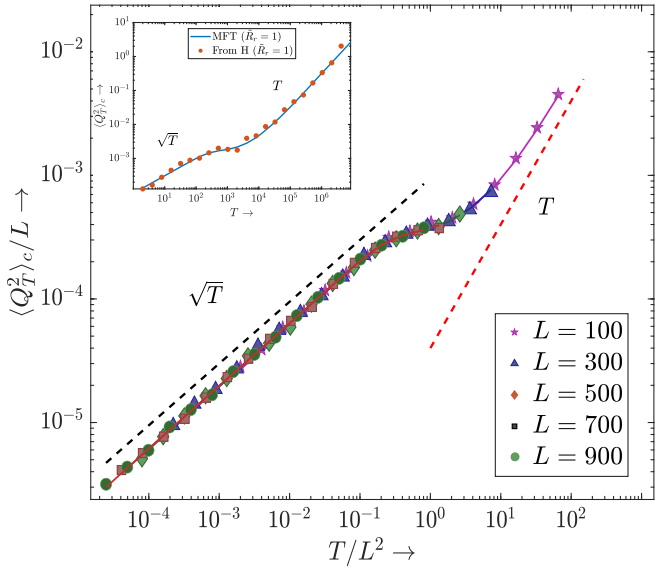

FIG. 3. The variance of number fluctuations is shown in rescaled coordinates, with time scaled as T/L^2 and variance as $\langle Q_T^2\rangle_c/L$. Curves for different system sizes collapse onto a single curve. For $T \ll T^*$, $\langle Q_T^2\rangle_c \sim \sqrt{T}$ (diffusive noise); for $T \gg T^*$, $\langle Q_T^2\rangle_c \sim T$ (reaction noise), confirming the predicted scaling. Inset: variance of Q_T from heterozygosity is plotted versus time for $L = 100$. Solid lines show MFT predictions from Eq. (22), and points show number-fluctuation estimates from Eq. (16). The plot exhibits two regimes: early diffusive-noise dominance and late reaction-noise dominance.

It is straightforward to analyze the scaling limits of the above expression: at short times ($T \ll T^*$) diffusive noise dominates and the sum converges to a scaling form $\langle Q_T^2\rangle_c \sim \sigma_d\sqrt{T}/\sqrt{2\pi D_d}$, while at long times ($T \gg T^*$) reaction noise prevails, yielding $\langle Q_T^2\rangle_c \sim \sigma_r T/8$, with a crossover timescale given by $T^* \sim 32\sigma_d^2/(\pi\sigma_r^2 D_d)$. The $\sqrt{T}$ scaling is typical of diffusive systems [24,51], while the linear T behavior is typical of reactive as well as active systems [57,63]. Interestingly, the short-time behavior of number fluctuations in the stepping-stone model is the same as the symmetric simple exclusion process (SSEP) [42,49,51,64,65], since in the absence of reaction dynamics the exchange rules are similar; however the fluctuations are reduced by a factor of $1/N$ compared to the SSEP. In contrast to the SSEP, where the crossover time in finite systems is set by the diffusive scale $\tau \sim L^2$; here, the crossover from $\sqrt{T}$ to T is independent of L and originates purely from the reaction dynamics rather than from finite-size effects (see Supplemental Material [35]).

Conclusions—Our analysis shows that both types of noise are essential for accurate predictions in spatially structured populations, particularly at short times when migration rates exceed reaction rates ($R_d \gg R_r$). This insight extends beyond population genetics to reaction-diffusion systems where transport and local reactions coexist [66–68]. While the classical stochastic Fisher equation [4,11,33] and related continuum models [8,69] focus on reaction noise (genetic drift), they miss the initial fluctuations when migration prevails. We provide quantifiable predictions for heterozygosity and number fluctuations that pinpoint the timescales over which diffusive noise controls early-time genetic demixing, a regime relevant to experiments where high migration in microbial expansions rapidly mixes alleles and suppresses local heterozygosity.

Our framework extends naturally to two-dimensional and heterogeneous landscapes, and it remains to be explored how diffusive noise alters fixation times and phase-separating dynamics. Quenched versus annealed initial conditions [24,51,52,54,70] can also be addressed within our MFT framework. Finally, since the noiseless equation (11) admits Fisher waves [10,16] with speeds set by initial conditions [71] and demographic noise renormalizes the front speed [11,69,72], strong diffusive noise may produce additional corrections; understanding its impact on Fisher wavefronts and genetic domain walls could clarify interface roughness and stability in biological and chemical systems [30,47,73].

Acknowledgments—We thank R. Benzi, S. Chakraborty, S. Prakash and S. D. Cengio for discussions. This project was funded by intramural funds at TIFR Hyderabad from the Department of Atomic Energy (DAE), Government of India, under Project Identification No. RTI4007.

Data availability—There are no publicly available research data or software supporting this manuscript. Requests for further information or data should be sent to the authors.

[1] W. Ewens, *Mathematical Population Genetics: Theoretical Introduction* (Springer, New York, NY, USA, 2004), Vol. 27.
[2] O. Hallatschek, P. Hersen, S. Ramanathan, and D. R. Nelson, Proc. Natl. Acad. Sci. U.S.A. **104**, 19926 (2007).
[3] N. Rana, P. Ghosh, and P. Perlekar, Phys. Rev. E **96**, 052403 (2017).
[4] S. Pigolotti, R. Benzi, P. Perlekar, M. H. Jensen, F. Toschi, and D. R. Nelson, Theor. Popul. Biol. **84**, 72 (2013).
[5] U. C. Täuber, in *Order, Disorder and Criticality: Advanced Problems of Phase Transitions and Complex Systems* (World Scientific, Singapore, 2025), pp. 67–115.
[6] J. Murray, *Mathematical Biology: An Introduction* (Springer, New York, 2002).
[7] M. Kimura and G. H. Weiss, Genetics **49**, 561 (1964).
[8] K. S. Korolev, M. Avlund, O. Hallatschek, and D. R. Nelson, Rev. Mod. Phys. **82**, 1691 (2010).
[9] T. Singha, P. Perlekar, and M. Barma, Phys. Rev. Res. **2**, 023412 (2020).
[10] R. A. Fisher, Ann. Eugen. **7**, 355 (1937).
[11] C. R. Doering, C. Mueller, and P. Smereka, Physica A (Amsterdam) **325**, 243 (2003).
[12] M. Raymond and M. Marquine, J. Evol. Biol. **7**, 315 (1994).
[13] R. M. May, J. A. Endler, and R. E. McMurtrie, Am. Nat. **109**, 659 (1975).
[14] T. Lenormand, Trends Ecol. Evol. **17**, 183 (2002).
[15] S. Jain and A. D. Bradshaw, Heredity **21**, 407 (1966).
[16] A. N. Kolmogorov and N. Piskunov, Bull. Moscow Univ. Math. Mech. **1**, 1 (1937).
[17] T. L. Duty, Ph. D. thesis, University of British Columbia, 2000.
[18] U. C. Täuber, M. Howard, and B. P. Vollmayr-Lee, J. Phys. A **38**, R79 (2005).
[19] S. Prakash, M. Barma, and K. Ramola, J. Stat. Mech. (2025) 103208 (2025).
[20] T. Agranov, S. Ro, Y. Kafri, and V. Lecomte, J. Stat. Mech. (2021) 083208.
[21] T. Bodineau and B. Derrida, J. Stat. Phys. **145**, 745 (2011).
[22] S. Jose, R. Dandekar, and K. Ramola, J. Stat. Mech. (2023) P083208.
[23] R. Mukherjee, S. Saha, T. Sadhu, A. Dhar, and S. Sabhapandit, Phys. Rev. E **111**, 024128 (2025).
[24] B. Derrida and A. Gerschenfeld, J. Stat. Phys. **137**, 978 (2009).
[25] L. Bertini, A. De Sole, D. Gabrielli, G. Jona-Lasinio, and C. Landim, Rev. Mod. Phys. **87**, 593 (2015).
[26] A. G. Thompson, J. Tailleur, M. E. Cates, and R. A. Blythe, J. Stat. Mech. (2011) P02029.
[27] O. M. Ghosh and B. H. Good, Proc. Natl. Acad. Sci. U.S.A. **119**, e2114931119 (2022).
[28] E. Khain and B. Meerson, J. Phys. A **46**, 125002 (2013).
[29] A. Lemarchand, J. Stat. Phys. **101**, 579 (2000).
[30] A. Lemarchand, I. Nainville, and M. Mareschal, Europhys. Lett. **36**, 227 (1996).
[31] C. Kim, A. Nonaka, J. B. Bell, A. L. Garcia, and A. Donev, J. Chem. Phys. **146**, 124110 (2017).
[32] R. E. Spinney and R. G. Morris, J. Phys. A **58**, 035004 (2025).
[33] K. Korolev and D. R. Nelson, Phys. Rev. Lett. **107**, 088103 (2011).
[34] P. A. P. Moran, Proc. Cambridge Philos. Soc. **54**, 60 (1958).
[35] See Supplemental Material at http://link.aps.org/supplemental/10.1103/xmbp-d85n for details, which includes Refs. [36,37].
[36] A. Prados, J. Brey, and B. Sánchez-Rey, J. Stat. Phys. **89**, 709 (1997).
[37] A. B. Bortz, M. H. Kalos, and J. L. Lebowitz, J. Comput. Phys. **17**, 10 (1975).
[38] A. Lefevre and G. Biroli, J. Stat. Mech. (2007) P07024.
[39] M. Doi, J. Phys. A **9**, 1465 (1976).
[40] L. Peliti, J. Phys. USSR **46**, 1469 (1985).
[41] B. Derrida, Phys. Rep. **301**, 65 (1998).
[42] H. Spohn, *Large Scale Dynamics of Interacting Particles* (Springer Science & Business Media, New York, 2012).
[43] J. Tailleur, J. Kurchan, and V. Lecomte, J. Phys. A **41**, 505001 (2008).

[44] A. De Masi, P. A. Ferrari, and J. Lebowitz, Phys. Rev. Lett. **55**, 1947 (1985).
[45] G. Jona-Lasinio, C. Landim, and M. Vares, Probab. Theory Relat. Fields **97**, 339 (1993).
[46] S. Saha and T. Sadhu, J. Stat. Mech. (2023) P073207.
[47] L. Pechenik and H. Levine, Phys. Rev. E **59**, 3893 (1999).
[48] P. C. Martin, E. D. Siggia, and H. Rose, Phys. Rev. A **8**, 423 (1973).
[49] B. Derrida, C. Enaud, C. Landim, and S. Olla, J. Stat. Phys. **118**, 795 (2005).
[50] D. S. Dean, J. Phys. A **29**, L613 (1996).
[51] P. Krapivsky and B. Meerson, Phys. Rev. E **86**, 031106 (2012).
[52] T. Banerjee, R. L. Jack, and M. E. Cates, Phys. Rev. E **106**, L062101 (2022).
[53] P. L. Krapivsky, K. Mallick, and T. Sadhu, J. Stat. Phys. **160**, 885 (2015).
[54] P. L. Krapivsky, K. Mallick, and T. Sadhu, Phys. Rev. Lett. **113**, 078101 (2014).
[55] K. Mallick, H. Moriya, and T. Sasamoto, Phys. Rev. Lett. **129**, 040601 (2022).
[56] R. Dandekar, P. Krapivsky, and K. Mallick, Phys. Rev. E **107**, 044129 (2023).
[57] S. Jose, A. Rosso, and K. Ramola, Phys. Rev. E **108**, L052601 (2023).
[58] L. Bertini, A. De Sole, D. Gabrielli, G. Jona-Lasinio, and C. Landim, Phys. Rev. Lett. **94**, 030601 (2005).
[59] L. Bertini, A. De Sole, D. Gabrielli, G. Jona-Lasinio, and C. Landim, J. Stat. Phys. **123**, 237 (2006).
[60] L. Bertini, A. De Sole, D. Gabrielli, G. Jona-Lasinio, and C. Landim, J. Stat. Mech. (2007) P07014.
[61] L. Bertini, A. De Sole, D. Gabrielli, G. Jona-Lasinio, and C. Landim, J. Stat. Phys. **135**, 857 (2009).
[62] R. Dandekar, P. Krapivsky, and K. Mallick, Phys. Rev. E **110**, 064153 (2024).
[63] T. Banerjee, S. N. Majumdar, A. Rosso, and G. Schehr, Phys. Rev. E **101**, 052101 (2020).
[64] D. G. Levitt, Phys. Rev. A **8**, 3050 (1973).
[65] R. Arratia, Ann. Probab. **11**, 362 (1983).
[66] J. V. Noble, Nature (London) **250**, 726 (1974).
[67] D. Campos, V. Méndez, and V. Ortega-Cejas, Bull. Math. Biol. **70**, 1937 (2008).
[68] L. Schimansky-Geier and C. Zülicke, Z. Phys. B **82**, 157 (1991).
[69] O. Hallatschek and K. S. Korolev, Phys. Rev. Lett. **103**, 108103 (2009).
[70] J. Cividini and A. Kundu, J. Stat. Mech. (2017) P083203.
[71] W. Van Saarloos, Phys. Rev. A **37**, 211 (1988).
[72] E. Brunet and B. Derrida, Phys. Rev. E **56**, 2597 (1997).
[73] O. Hallatschek and D. R. Nelson, Evolution (Lawrence, Kans.) **64**, 193 (2010).